PHYSICAL REVIEW B **75**, 081101(R) (2007)

Exact Green's functions for the two-site Hubbard-Holstein Hamiltonian

Mona Berciu
Department of Physics and Astronomy, University of British Columbia, Vancouver, Canada, BC V6T 1Z1
(Received 14 November 2006; revised manuscript received 7 January 2007; published 5 February 2007)

We derive exactly all Green's functions for the two-site Hubbard-Holstein model. We then study the bipolaron phase diagram, with emphasis on its unbinding into two polarons and on the crossover from a two-site to a one-site bipolaron. The results are relevant for infinite-size systems.

DOI: 10.1103/PhysRevB.75.081101 PACS number(s): 71.38.−k, 72.10.Di, 63.20.Kr

It is well known that electron-phonon coupling mediates an effective attraction between electrons; this is responsible for Cooper-pair formation in conventional superconductors. With electron-phonon coupling, electrons also become dressed by phonon clouds. The resulting polarons can have properties quite different from those of bare electrons. If electron-electron repulsion is screened, polarons tend to bind into bipolarons due to the phonon-mediated attraction. The interplay between this effective attraction and the electron-electron repulsion is of significant interest for understanding the properties of materials where polaronic and bipolaronic effects are known to be important—e.g., transition-metal-oxides[1] and conjugated polymers.[2] For cuprates there is growing evidence that electron-phonon interactions are rather important,[3] and this is well known to be the case for manganites.[4]

In this context, finding exact solutions even for simpler models is useful, as they allow us to understand regions in parameter space where perturbation theory fails. Here we derive analytically all Green's functions of the two-site Hubbard-Holstein (HH) model, with emphasis on the bipolaron. These results are of interest for materials with highly polarizable small clusters, such as Ti-Ti pairs in Ti_4O_7 and V-V pairs in $Na_xV_2O_5$. As we argue below, they are also directly relevant for understanding polaron and bipolaron behavior on infinite lattices. Previously, the two-site HH model was studied by numerical[5] and variational[6] means. The analytical solution for the polaron Green's function was recently found.[7]

The two-site Hubbard-Holstein Hamiltonian is

$$\mathcal{H} = \mathcal{H}_{el} + \mathcal{H}_{ph} + V_{el\text{-}ph}, \tag{1}$$

where the electronic part

$$\mathcal{H}_{el} = -t\sum_{\sigma}(c^{\dagger}_{1,\sigma}c_{2\sigma} + \text{H.c.}) + U(n_{1\uparrow}n_{1\downarrow} + n_{2\uparrow}n_{2\downarrow}) \tag{2}$$

describes hopping and the on-site Hubbard repulsion,

$$\mathcal{H}_{ph} = \Omega(b^{\dagger}_1 b_1 + b^{\dagger}_2 b_2)$$

describes longitudinal vibrations of the two sites, and

$$V_{el-ph} = g[n_1(b^{\dagger}_1 + b_1) + n_2(b^{\dagger}_2 + b_2)]$$

is the Holstein electron-phonon coupling. Here $n_{i\sigma}=c^{\dagger}_{i\sigma}c_{i\sigma}$, $n_i=\Sigma_{\sigma}n_{i\sigma}$ are electron occupation numbers, and we set $\hbar=1$. Using relative and center-of-mass (c.m.) bosons $b=(b_1-b_2)/\sqrt{2}$, $B=(b_1+b_2)/\sqrt{2}$, we rewrite $\mathcal{H}_{ph}+V_{el\text{-}ph}=\Omega(B^{\dagger}B+b^{\dagger}b)+g/\sqrt{2}[(n_1+n_2)(B^{\dagger}+B)+(n_1-n_2)(b^{\dagger}+b)]$. In any N-electron state the c.m. part is $\Omega B^{\dagger}B+Ng(B^{\dagger}+B)/\sqrt{2}=\Omega\bar{B}^{\dagger}\bar{B}-N^2g^2/(2\Omega^2)$, where $\bar{B}=B+gN/(\sqrt{2}\Omega)=XBX^{\dagger}$ with $X=\exp[-gNB^{\dagger}/(\sqrt{2}\Omega)]$. From now on we assume that the c.m. motion is frozen in its ground state (g.s.) $|\bar{0}\rangle\sim X|0\rangle$, so that $E_{\text{c.m.}}=-N^2g^2/(2\Omega^2)$. This simply shifts all spectra. The remaining terms are

$$\mathcal{H}_{ph} + V_{el\text{-}ph} = \Omega b^{\dagger}b + \frac{g}{\sqrt{2}}(n_1 - n_2)(b^{\dagger} + b). \tag{3}$$

As a first step to finding bipolaron Green's functions, we list the two-electron eigenstates of $\mathcal{H}_{el}$. The three triplet states $|1,1\rangle=c^{\dagger}_{1\uparrow}c^{\dagger}_{2\uparrow}|0\rangle$, $|1,0\rangle=(c^{\dagger}_{1\uparrow}c^{\dagger}_{2\downarrow}+c^{\dagger}_{1\downarrow}c^{\dagger}_{2\uparrow})/\sqrt{2}|0\rangle$, and $|1,-1\rangle=c^{\dagger}_{1\downarrow}c^{\dagger}_{2\downarrow}|0\rangle$ are degenerate, $\mathcal{H}_{el}|1,m\rangle=0$. Since $(n_1-n_2)|1,m\rangle=0$, Eq. (3) shows that the triplet sector of the Hilbert space is not coupled to b bosons and so its spectrum is unchanged. We ignore these states from now on. The singlet $|s\rangle=(c^{\dagger}_{1\uparrow}c^{\dagger}_{2\downarrow}-c^{\dagger}_{1\downarrow}c^{\dagger}_{2\uparrow})/\sqrt{2}|0\rangle$ and doubly occupied states $|\pm\rangle=(c^{\dagger}_{1\uparrow}c^{\dagger}_{1\downarrow}\pm c^{\dagger}_{2\uparrow}c^{\dagger}_{2\downarrow})/\sqrt{2}|0\rangle$ give rise to the remaining three eigenstates

$$\mathcal{H}_{el}|-\rangle = U|-\rangle, \quad \mathcal{H}_{el}|s\pm\rangle = E_{\pm}|s\pm\rangle,$$

where

$$|s-\rangle = \cos\theta|s\rangle + \sin\theta|+\rangle, \quad |s+\rangle = \sin\theta|s\rangle - \cos\theta|+\rangle,$$

$$E_{\pm} = \frac{U \pm \sqrt{U^2+16t^2}}{2}, \quad \cos\theta = \sqrt{\frac{1}{2}\left(1 + \frac{U}{\sqrt{U^2+16t^2}}\right)}.$$

For $U>0$ and ignoring the triplet eigenstates, $|s-\rangle$ is the ground state, followed by $|-\rangle$ and $|s+\rangle$ as excited states.

For these states, $(n_1-n_2)|s-\rangle=2\sin\theta|-\rangle$, $(n_1-n_2)|s+\rangle=-2\cos\theta|-\rangle$, and $(n_1-n_2)|-\rangle=2(\sin\theta|s-\rangle-\cos\theta|s+\rangle)$. Coupling to the b bosons mixes these states, therefore giving rise to new bipolaron eigenstates. To find their eigenvalues and eigenfunctions, we calculate the bipolaron Green's functions, which we define as

$$\mathcal{G}^{n,m}_{f,i}(\omega) = \langle f|b^n\hat{G}(\omega)b^{\dagger,m}|i\rangle, \tag{4}$$

where $|i\rangle$ and $|f\rangle$ are any of the $|s\pm\rangle$ and $|-\rangle$ eigenstates, and $\hat{G}(\omega)=(\omega-\mathcal{H}+i\eta)^{-1}$ is the Green operator. Note that to account for the c.m. contribution, we must replace $\omega\rightarrow\omega-E_{\text{c.m.}}$. We do this for all the results we show below.

Using a Lehmann representation in terms of the true bipolaron eigenstates $\mathcal{H}|2,\alpha\rangle=E_{2,\alpha}|2,\alpha\rangle$ results in

$$\mathcal{G}_{f,i}^{n,m}(\omega) = \sum_{\alpha} \frac{\langle f|b^n|2,\alpha\rangle\langle 2,\alpha|b^{\dagger,m}|i\rangle}{\omega - E_{2,\alpha} + i\eta}, \tag{5}$$

showing that poles mark the bipolaron spectrum and wave functions can be extracted from the residues. Also, $\mathcal{G}_{f,i}(\omega,T)=(1-e^{-\beta\omega})\Sigma_{n=0}^{\infty}\frac{e^{-\beta n\omega}}{n!}\mathcal{G}_{f,i}^{n,n}(\omega+n\Omega)$ are temperature-dependent bipolaron Green's functions.

We show in detail the derivation of $\mathcal{G}_{-,-}^{n,m}(\omega)$ and $\mathcal{G}_{-,s\pm}^{n,m}(\omega)$. Other Green's functions are derived similarly. The calculation is based on Dyson's identity $\hat{G}(\omega)=\hat{G}_0(\omega)+\hat{G}(\omega)V_{el\text{-}ph}\hat{G}_0(\omega)$, where $\hat{G}_0(\omega)=(\omega-\mathcal{H}_{el}-\mathcal{H}_{ph}+i\eta)^{-1}$ has the eigenvalues $\hat{G}_0(\omega)b^{\dagger,m}|s\pm\rangle=g_{s\pm}(\omega-m\Omega)b^{\dagger,m}|s\pm\rangle$ and $\hat{G}_0(\omega)b^{\dagger,m}|-\rangle=g_{-}(\omega-m\Omega))b^{\dagger,m}|-\rangle$ with

$$g_{s\pm}(\omega) = (\omega - E_{\pm} + i\eta)^{-1}, \quad g_{-}(\omega) = (\omega - U + i\eta)^{-1}$$

being the two-electron Green's functions for zero coupling. For later convenience, we also introduce

$$g(\omega) = g_{s-}(\omega)\sin^2\theta + g_{s+}(\omega)\cos^2\theta. \tag{6}$$

First, we define

$$F_{nm} = \begin{cases} \langle -|b^n\hat{G}(\omega)b^{\dagger,m}|-\rangle, & \text{if } n-m \text{ even}, \\ \langle -|b^n\hat{G}(\omega)b^{\dagger,m}|+\rangle, & \text{if } n-m \text{ odd}; \end{cases} \tag{7}$$

i.e., $F_{nm}=\sin\theta\mathcal{G}_{-,s-}^{n,m}(\omega)-\cos\theta\mathcal{G}_{-,s+}^{n,m}(\omega)$ if $n-m$ is odd. Using Dyson's identity, we find the recursion relations

$$F_{nm} = \delta_{nm}n!f(\omega) + g_{nm}(\omega)[mF_{n,m-1} + F_{n,m+1}], \tag{8}$$

where $f(\omega)=g_{-}(\omega-n\Omega)$ and

$$g_{nm}(\omega) = \begin{cases} \sqrt{2}gg_{-}(\omega-m\Omega), & \text{if } n-m \text{ even}, \\ \sqrt{2}gg(\omega-m\Omega), & \text{if } n-m \text{ odd}. \end{cases} \tag{9}$$

Equations (8) is solved in terms of continued fractions.[8] For $m<n$, iterations starting from $m=0$ show that $F_{n,m-1}=A_{n,m}F_{n,m}$, while for $m>n$, iterations starting from $m\gg n$ show that $F_{n,m+1}=B_{n,m}F_{n,m}$, where

$$A_{n,m}(\omega) = \cfrac{g_{n,m-1}(\omega)}{1-\cfrac{(m-1)g_{n,m-1}(\omega)g_{n,m-2}(\omega)}{1-\cfrac{(m-2)g_{n,m-2}(\omega)g_{n,m-3}(\omega)}{1-\cdots}}}, \tag{10}$$

$$B_{n,m}(\omega) = \cfrac{(m+1)g_{n,m+1}(\omega)}{1-\cfrac{(m+2)g_{n,m+1}(\omega)g_{n,m+2}(\omega)}{1-\cfrac{(m+3)g_{n,m+2}(\omega)g_{n,m+3}(\omega)}{1-\cdots}}} \tag{11}$$

are finite and infinite continued fractions, respectively. Using $F_{n,n-1}$ and $F_{n,n+1}$ in Eq. (8) with $n=m$ then gives

$$F_{n,n} = \frac{n!f(\omega)}{1-g_{nn}(\omega)[nA_{n,n}(\omega)+B_{n,n}(\omega)]}. \tag{12}$$

Then, if $m<n$, $F_{n,m}=A_{n,m+1}A_{n,m+2}\cdots A_{n,n}F_{n,n}$ while if $m>n$, $F_{n,m}=B_{n,m-1}B_{n,m-2}\cdots B_{n,n}F_{n,n}$.

$\mathcal{G}_{-,-}^{n,m}(\omega)=F_{nm}$ if $n-m$ is even. Otherwise, Dyson's identity gives

$$\begin{aligned}\langle -|b^n\hat{G}(\omega)b^{\dagger,m}|s\rangle &= \cos\theta\mathcal{G}_{-,s-}^{n,m}(\omega) + \sin\theta\mathcal{G}_{-,s+}^{n,m}(\omega) \\ &= g\sqrt{2}\sin\theta\cos\theta[g_{s-}(\omega-m\Omega) \\ &\quad - g_{s+}(\omega-m\Omega)][mF_{n,m-1}+F_{n,m+1}],\end{aligned}$$

which is known. Combining this with the also known $F_{nm}=\sin\theta\mathcal{G}_{-,s-}^{n,m}(\omega)-\cos\theta\mathcal{G}_{-,s+}^{n,m}(\omega)$ then gives all $\mathcal{G}_{-,s\pm}^{n,m}(\omega)$ for odd $n-m$. Finally, interchanging the expressions for even and odd cases in the definition of F_{nm}, it is straightforward to show that $\mathcal{G}_{-,-}^{n,m}(\omega)=0$ if $n-m$ is odd and $\mathcal{G}_{-,s\pm}^{n,m}(\omega)=0$ if $n-m$ is even. This completes their derivation. Other bipolaron Green's functions are found similarly, starting with the appropriate matrix elements in the equivalent of Eq. (7). We list here only the "diagonal" elements:

$$\mathcal{G}_{-,-}^{n,n}(\omega) = \frac{n!g_{-}(\omega-n\Omega)}{1-g_{nn}(\omega)[nA_{n,n}(\omega)+B_{n,n}]}, \tag{13}$$

$$\begin{aligned}\mathcal{G}_{s-,s-}^{n,n}(\omega) &= n!g_{s-}(\omega-n\Omega) \\ &\times\left[1+\frac{\sin^2\theta\sqrt{2}gg_{s-}(\omega-n\Omega)[n\tilde{A}_{n,n}(\omega)+\tilde{B}_{n,n}(\omega)]}{1-\tilde{g}_{nn}(\omega)[n\tilde{A}_{n,n}(\omega)+\tilde{B}_{n,n}(\omega)]}\right],\end{aligned} \tag{14}$$

$$\begin{aligned}\mathcal{G}_{s+,s+}^{n,n}(\omega) &= n!g_{s+}(\omega-n\Omega) \\ &\times\left[1+\frac{\cos^2\theta\sqrt{2}gg_{s+}(\omega-n\Omega)[n\tilde{A}_{n,n}(\omega)+\tilde{B}_{n,n}(\omega)]}{1-\tilde{g}_{nn}(\omega)[n\tilde{A}_{n,n}(\omega)+\tilde{B}_{n,n}(\omega)]}\right].\end{aligned} \tag{15}$$

$\tilde{A}_{n,m}(\omega)$ and $\tilde{B}_{n,m}(\omega)$ are given by Eqs. (10) and (11) but with g_{nm} replaced by $\tilde{g}_{nm}$, where

$$\tilde{g}_{nm}(\omega) = \begin{cases} \sqrt{2}gg(\omega-m\Omega), & \text{if } n-m \text{ even}, \\ \sqrt{2}gg_{-}(\omega-m\Omega), & \text{if } n-m \text{ odd}. \end{cases} \tag{16}$$

The Green's functions for the $N=1$ and $N=3$ electron cases are found similarly. We quickly summarize the $N=1$ (polaron) case; $N=3$ can be mapped onto it. The spin of the electron is now irrelevant, and we ignore it. $\mathcal{H}_{el}$ has two eigenstates $|e/o\rangle=(c_1^{\dagger}\pm c_2^{\dagger})/\sqrt{2}|0\rangle$, and $V_{el\text{-}ph}$ couples one to the other. Proceeding as before, we find all the polaron Green's functions—in particular,

$$G_{e,e}^{n,n}(\omega) = \langle e|b^n\hat{G}(\omega)b^{\dagger,n}|e\rangle = \frac{n!g_e(\omega-n\Omega)}{1-\bar{g}_{nn}(\omega)[n\bar{A}_{n,n}+\bar{B}_{n,n}]},$$

where again $\bar{A}_{n,n}$ and $\bar{B}_{n,n}$ are given by Eqs. (10) and (11), but now with $g_{nm}(\omega)\to\bar{g}_{nm}(\omega)$, where

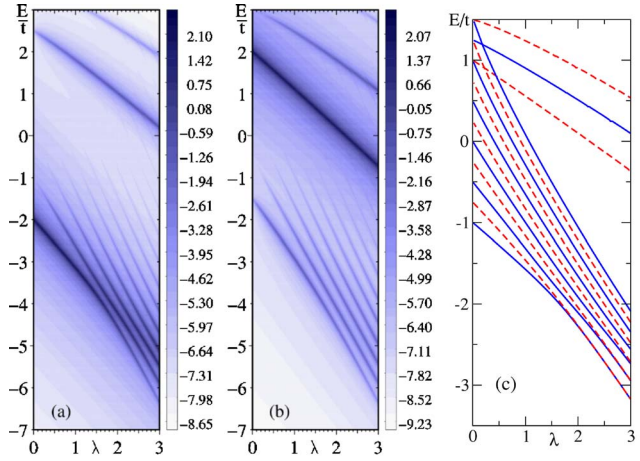

FIG. 1. (Color online) (a) $-\frac{1}{\pi}\,\mathrm{Im}\,G^{0,0}_{e,e}(\omega)$, (b) $-\frac{1}{\pi}\,\mathrm{Im}\,G^{0,0}_{o,o}(\omega)$, and (c) poles of $G^{0,0}_{e,e}(\omega)$ (solid lines) and $G^{0,0}_{o,o}(\omega)$ (dashed lines) as a function of $\lambda=g^2/(t\Omega)$, for $t=2$, $\Omega=0.5$.

$$\bar{g}_{nm}(\omega)=\begin{cases} g g_e(\omega-m\Omega)/\sqrt{2}, & \text{if } n-m \text{ even},\\ g g_o(\omega-m\Omega)/\sqrt{2}, & \text{if } n-m \text{ odd}. \end{cases} \tag{17}$$

$g_e(\omega)=(\omega+t+i\eta)^{-1}$ and $g_o(\omega)=(\omega-t+i\eta)^{-1}$ are the free one-electron Green's functions. $G^{n,n}_{o,o}(\omega)$ is obtained by exchanging $g_e(\omega)\leftrightarrow g_o(\omega)$ (or $t\rightarrow -t$) everywhere.

Let us focus on the $n=0$ case—i.e., the $T=0$ polaron Green's functions. The different denominators of $G^{0,0}_{e,e}(\omega)$ and $G^{0,0}_{o,o}(\omega)$ signal two distinct sets of eigenstates. Indeed, in Figs. 1(a) and 1(b) we plot the $T=0$ spectral weights $-\frac{1}{\pi}\,\mathrm{Im}\,G^{0,0}_{e,e}(\omega)$ and $-\frac{1}{\pi}\,\mathrm{Im}\,G^{0,0}_{o,o}(\omega)$ *on a logarithmic scale*, so that peaks with small weight are visible. In Fig. 1(c) we trace a few eigenstates versus the effective coupling $\lambda=g^2/(t\Omega)$ (the coordination number $2d$ of infinite lattices is here replaced by 1). Consider first $g=0$. Here we have two sets of states with energies $\pm t+n\Omega$ (only the $\pm t$ peaks are seen in $G^{0,0}$). For small g, mixing gives some weight to the other eigenstates and all become visible. Because $G^{n,m}_{e,e}(\omega)=G^{n,m}_{o,o}(\omega)=0$ if $n-m$ is odd, eigenstates are either of type $\Sigma_n(\alpha_n b^{\dagger,2n}|e\rangle+\beta_n b^{\dagger,2n+1}|o\rangle)$ [these are shown by $G^{n,n}_{e,e}(\omega)$] or $\Sigma_n(\gamma_n b^{\dagger,2n+1}|e\rangle+\delta_n b^{\dagger,2n}|o\rangle)$ [these are shown by $G^{n,n}_{o,o}(\omega)$]. As λ increases, interactions lower all energies. For $\lambda\sim 1.5$, the two lowest states become almost degenerate, indicating that small, one-site polarons have been formed (the two states are the symmetric and antisymmetric combinations of Lang-Firsov-type solutions). For larger λ, the *low-energy spectrum* is similar to that of a polaron on an infinite lattice. This also has kinetic energy, but the bandwidth is exponentially suppressed and this contribution is negligible.[11,12]

The same holds true for a bipolaron. This enables us to extract information about bipolaron behavior in the strong-coupling limit, which is of direct relevance for infinite systems. We begin by studying the bipolaron ground state. In Fig. 2(a), we plot the g.s. [lowest pole of $\mathcal{G}^{0,0}_{s-,s-}(\omega)$] and the first excited state [lowest pole of $\mathcal{G}^{0,0}_{-,-}(\omega)$] versus λ, for $t=2$, $\Omega=0.5$, and $U=8$. At $g=0$, the g.s. has energy E_-, while $\mathcal{G}^{0,0}_{-,-}(\omega)$ shows only a pole at $+U$ (not shown). For finite

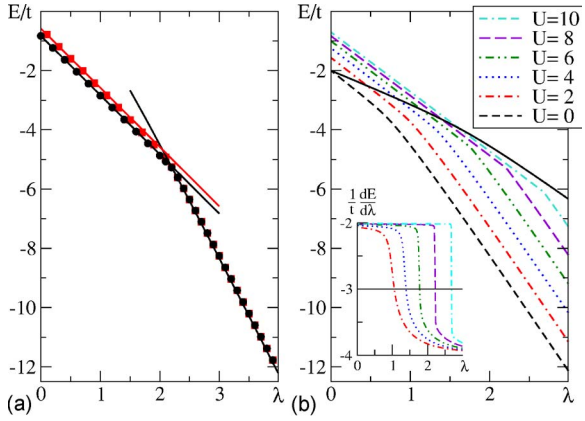

FIG. 2. (Color online) Left: g.s. (circles) and first excited state (squares) bipolaron energies vs λ, for $U=8$. Lines are fits described in the text. Right: g.s. energy (and its derivative with λ, inset) for $U=0,2,4,6,8,10$. The solid line is twice the polaron g.s. energy. In all cases $t=2$, $\Omega=0.5$.

small g, mixing between $|-\rangle$ and $b^\dagger|s-\rangle$ creates a state of small weight and energy $\approx E_-+\Omega$, visible in $\mathcal{G}^{0,0}_{-,-}(\omega)$. This is the first excited state at all finite g (like for the polaron, there is an infinite sequence of higher-energy states which we do not show here). As the coupling increases, the energies of both states decrease. Figure 2(a) shows two regimes: for $\lambda<2$, both energies decrease with almost the same slope. The energies are well fitted by E_--2g^2/Ω and $E_-+\Omega-2g^2/\Omega$, respectively [see Fig. 2(a)]. This shows that here the bipolaron g.s. consists mostly of a two-site singlet (so a U penalty for double occupancy is avoided) and each electron creates its own polaron cloud on its site, so that energy is lowered by $2(-g^2/\Omega)$. However, for larger λ, it becomes advantageous to have both electrons on one site. Here, the two eigenstates become almost degenerate, corresponding again to symmetric and antisymmetric combinations of bipolarons on the two sites. The energy is well fitted by $U-4g^2/\Omega-t^2\Omega/g^2$ [see Fig. 2(a)], where the first term is the penalty for double occupancy, the second term is the energy $-(2g)^2/\Omega$ of the phonon cloud created when both electrons are at the same site, and the third term is a perturbational correction coming from virtual hopping of one electron to the other site, leaving the phonon cloud behind. The crossover from the two-site bipolaron (called $S1$; see Refs. 9 and 10) at smaller λ to a single-site bipolaron (called $S0$) at larger λ is quite sharp especially for larger U, as can be seen in Fig. 2(b). When it occurs at a fairly large λ, this value should agree well with the value for this crossover found in numerical studies of infinite lattices. In the infinite lattice both types of bipolarons also have (different) kinetic energies associated with their center-of-mass translation; however, at large λ the kinetic energies are exponentially small[9–11] and should not significantly shift the crossover.

Interestingly, even the unbinding of the $S1$ bipolaron into two polarons, at a smaller λ, can be traced accurately using these two-site model results. In Fig. 2(b), the solid line shows twice the g.s. energy of a polaron. At small λ, two polarons are energetically more favorable than a $S1$ bipolaron, suggesting bipolaron unbinding in an infinite system.

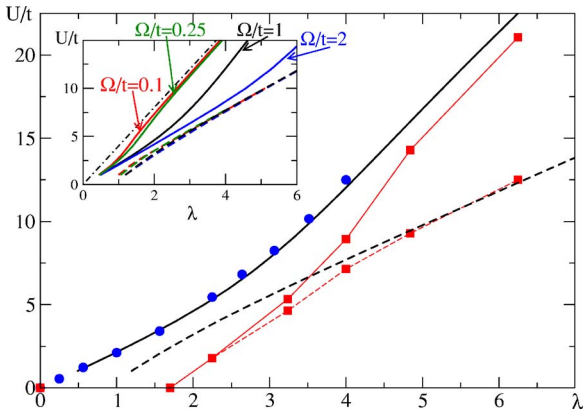

FIG. 3. (Color online) Bipolaron phase diagram: unbinding (solid line) and $S1 \rightarrow S0$ crossover (dashed line). Circles are one-dimensional (1D) results (Ref. 9) for unbinding, squares are 2D results (Ref. 10), for $t=\Omega=1$. Inset: same for $\Omega/t=0.1, 0.25, 1, 2$ (red/gray, green/light gray, black, blue/dark gray).

Again, we expect this unbinding value to be quite accurate as long as it is in the range where polarons and bipolarons are very heavy.

Based on these considerations, we draw a phase diagram for bipolarons, shown in Fig. 3. We use $t=\Omega=1$ so we can compare with results obtained numerically for infinite 1D and 2D Hubbard-Holstein models.[9,10] There is good agreement with the 1D values for the unbinding line (the $S1 \rightarrow S0$ crossover was not studied numerically in Ref. 9). The agreement with the 2D results is poorer at weaker couplings, but acceptable at stronger couplings. For the $S1 \rightarrow S0$ crossover, this may be due to a different "definition" of the crossover [we use the change of slope of the g.s. energy (see inset of Fig. 2), while they use the change in the effective mass]. As U decreases, the crossover becomes less sharp, so different criteria may give quite different results. The other important point is that the two-site HH predictions are relevant for an infinite system only if masses are exponentially large. The crossover to heavy polarons occurs for $g^2/(\Omega t) \approx 2d$.[11] This suggests that the two-site HH predictions should not be taken seriously for $\lambda < 2$ (in 1D) and $\lambda < 4$ (in 2D).

The $S1 \rightarrow S0$ crossover does not vary much with Ω/t (dashed lines in the inset of Fig. 3). It stays close to the expected strong-coupling asymptotic value[9,10] $U - 4g^2/\Omega \approx -2g^2/\Omega \rightarrow U/t \approx 2\lambda$. However, the unbinding line does change significantly. As $\Omega/t \rightarrow 0$, it approaches the expected strong-coupling asymptotic value $U/t=4\lambda$ (dash-dotted line). For larger Ω/t, the unbinding line initially stays quite close to the $S0 \rightarrow S1$ crossover until larger λ values when it moves towards $U/t=4\lambda$. Thus, the region of parameter space inhabited by $S1$ bipolarons expands as Ω/t decreases, as also noted in Ref. 13.

In conclusion, it was shown that all Green's functions for the two-site Hubbard-Holstein model can be derived analytically in terms of continued fractions. From these, one can calculate virtually any quantity of interest, such as eigenenergies, wave functions, phonon statistics in different states, temperature dependence, etc. These results are relevant for materials containing two-site clusters and can also be used as a starting point for cluster perturbation theories.[14] Interestingly, they also allow us to understand aspects of polaron and bipolaron physics in infinite systems at strong couplings.

This work was supported by the A. P. Sloan Foundation, CIAR Nanoelectronics, NSERC, and CFI.

[1] C. Schlenker, in *Physics of Disordered Materials*, edited by D. Adler, H. Fritzche, and S. Ovshinski (Plenum, New York, 1985).
[2] O. Gunnarsson, Rev. Mod. Phys. **69**, 575 (1997).
[3] A. Lanzara, N. L. Saini, M. Brunelli, F. Natali, A. Bianconi, P. G. Radaelli, and S. W. Cheong, Phys. Rev. Lett. **81**, 878 (1998); K. M. Shen, F. Ronning, D. H. Lu, W. S. Lee, N. J. C. Ingle, W. Meevasana, F. Baumberger, A. Damascelli, N. P. Armitage, L. L. Miller, Y. Kohsaka, M. Azuma, M. Takano, H. Takagi, and Z.-X. Shen, *ibid.* **93**, 267002 (2004); Jinho Lee, K. Fujita, K. McElroy, J. A. Slezak, M. Wang, Y. Aiura, H. Bando, M. Ishikado, T. Masui, J.-X. Zhu, A. V. Balatsky, H. Eisaki, S. Uchida, and J. C. Davis, Nature (London) **442**, 546 (2006).
[4] D. M. Edwards, Adv. Phys. **51**, 1259 (2002).
[5] E. V. L. de Mello and J. Ranninger, Phys. Rev. B **55**, 14872 (1997); J. Ranninger and U. Thibblin, *ibid.* **45**, 7730 (1992).
[6] M. Acquarone, J. R. Iglesias, M. A. Gusmao, C. Noce, and A. Romano, Phys. Rev. B **58**, 7626 (1998).
[7] Rongsheng Han, Zijing Lin, and Kelin Wang, Phys. Rev. B **65**, 174303 (2002); S. Paganelli and S. Ciuchi, J. Phys.: Condens. Matter **18**, 7669 (2006).
[8] V. S. Viswanath and G. Müller, *The Recursion Method* (Springer-Verlag, Berlin, 1994).
[9] J. Bonca, T. Katrasnik, and S. A. Trugman, Phys. Rev. Lett. **84**, 3153 (2000).
[10] A. Macridin, G. A. Sawatzky, and M. Jarrell, Phys. Rev. B **69**, 245111 (2004).
[11] G. L. Goodvin, M. Berciu, and G. A. Sawatzky, Phys. Rev. B **74**, 245104 (2006).
[12] M. Hohenadler, M. Aichhorn, and W. von der Linden, Phys. Rev. B **71**, 014302 (2005).
[13] M. Hohenadler and W. von der Linden, Phys. Rev. B **71**, 184309 (2005).
[14] D. Sénéchal, D. Perez, and D. Plouffe, Phys. Rev. B **66**, 075129 (2002).